Journal of Neuroscience Methods 175 (2008) 148–153

Contents lists available at ScienceDirect

Journal of Neuroscience Methods

journal homepage: www.elsevier.com/locate/jneumeth

Overt foot movement detection in one single Laplacian EEG derivation

Teodoro Solis-Escalante*, Gernot Müller-Putz, Gert Pfurtscheller

Laboratory of Brain-Computer Interfaces, Institute for Knowledge Discovery, Graz University of Technology, Krenngasse 37, 8010 Graz, Austria

ARTICLE INFO

Article history:
Received 8 May 2008
Received in revised form 29 July 2008
Accepted 29 July 2008

Keywords:
Event-related (de)synchronization
Asynchronous brain–computer interface
Support vector machines

ABSTRACT

In this work one single Laplacian derivation and a full description of band power values in a broad frequency band are used to detect brisk foot movement execution in the ongoing EEG. Two support vector machines (SVM) are trained to detect the event-related desynchronization (ERD) during motor execution and the following beta rebound (event-related synchronization, ERS) independently. Their performance is measured through the simulation of an asynchronous brain switch. ERS (true positive rate = 0.74 ± 0.21) after motor execution is shown to be more stable than ERD (true positive rate = 0.21 ± 0.12). A novel combination of ERD and post-movement ERS is introduced. The SVM outputs are combined with a product rule to merge ERD and ERS detection. For this novel approach the average information transfer rate obtained was 11.19 ± 3.61 bits/min.

1. Introduction

A brain–computer interface (BCI) transforms signals generated in the human brain into commands that can control devices or applications. In this way, a BCI provides a non-muscular communication channel (Wolpaw et al., 2002). The original goal of BCI systems is to help patients with severe motor disabilities and to improve their quality of life (Birbaumer et al., 1999; Pfurtscheller et al., 2005a; Neuper et al., 2003). Nowadays, non-invasive EEG-based BCIs are increasing their importance as an alternative control technology for able-bodied subjects. Possible applications include the use of such systems for user authentication through a “pass-thought”, a subject-specific brain pattern that is used instead of an alphanumeric password (Thorpe et al., 2005), controlling computer games (Müller-Putz et al., 2007a) and multimedia applications (Scherer et al., 2007). Important in all these applications is the suitability of the BCI system for use at home; this requires a sensor montage that is easy to apply and a simple strategy to set-up a classifier that is able to detect “thought”-related changes in the ongoing EEG. One way to achieve this is to use a reduced set of electrodes.

Motor imagery-based BCIs can be realized either with a large set of electrodes and highly sophisticated spatial filtering methods (Blankertz et al., 2007) or with a reduced number of subject-specific bipolar channels (Leeb et al., 2007). Here we report on a novel approach, namely the use of physiological knowledge about the dynamics of sensorimotor rhythms in a motor task to classify movement-related EEG changes in one single Laplacian derivation. Before imagery-related data are analyzed, motor execution data are subject to detailed investigation. Both functional magnetic resonance imaging (Lotze et al., 1999; Gerardin et al., 2000; Ehrsson et al., 2003) and EEG (Pfurtscheller and Lopes da Silva, 1999b) studies have shown that similar neural structures are activated during motor execution and imagination of the same movement without motor output.

The physiological phenomena of interest are the event-related desynchronization (ERD) of sensorimotor rhythms, terminated by a short-lasting beta event-related synchronization (ERS, beta rebound), observed during both covert and overt limb movement (Salmelin et al., 1995; Pfurtscheller and Lopes da Silva, 1999a; Neuper and Pfurtscheller, 2001; Pfurtscheller et al., 2005b), passive movement (limb movement without any efferent information flow) as well as movement induced by functional electrical stimulation (Müller et al., 2003). The beta rebound displays somatotopically specific patterns and coincides with a reduced excitability level of motor cortex neurons (Chen et al., 1998). It might be related to a deactivated state of motor cortex networks and/or a resetting mechanism of previously activated networks (Hari, 2006).

In this study we address the following questions:

(1) Is it possible to detect brisk foot movements in one single Laplacian EEG derivation when either ERD or ERS is considered?
(2) Does the performance improve when information about both phenomena (ERD and ERS) is combined?

* Corresponding author. Tel.: +43 316 873 5317.
E-mail address: teodoro.solisescalante@tugraz.at (T. Solis-Escalante).

0165-0270/$ – see front matter © 2008 Elsevier B.V. All rights reserved.
doi:10.1016/j.jneumeth.2008.07.019

2. Materials and methods

2.1. Data description

EEG recordings from 10 healthy subjects (6 males and 4 females aged 24.6 ± 1.4 years, median 24 years) were made during the execution of a cue-based foot movement. Each subject performed three runs with 30 trials each. All runs were conducted on the same day with several minutes in between. In the paradigm, a cross was presented at $t = 0$ s; then at $t = 2$ s, an arrow pointing downwards was displayed as a cue and the subject was asked to perform a brisk movement (dorsiflexion) of both feet. The movement duration was about 1 s. At $t = 3.25$ s the cue, and at $t = 6$ s the cross, disappeared. After the end of the trial ($t = 7.5$ s), a random inter-trial interval, with a maximum duration of 1 s, was presented. Sixteen Ag–AgCl electrodes placed over the sensorimotor area were used to record monopolar EEG signals (Guger Technologies, Graz, Austria) with a sampling frequency of 250 Hz. From these data, one small Laplacian derivation (Hjorth, 1975) at electrode position Cz was computed using orthogonal neighbor electrodes (anterior, posterior and both lateral). Further details about the data collection can be found in Müller-Putz et al. (2007b). The quality of the data was verified with the computation of the mean and the standard deviation of all trials in all runs. Three subjects were discarded for further analysis because they displayed no significant post-movement beta rebound.

2.2. Pattern description

Each trial was analyzed using time segments of 1 s length with an overlap of 500 ms from $t = -1$ to 9 s relative to the start of a trial (cue was presented at $t = 2$ s). The spectral description of each segment was computed by means of logarithmic band power: (i) band-pass filtering (62 order FIR), (ii) squaring the value of each sample, (iii) averaging all samples within the time segment and (iv) applying the logarithm function. A feature vector of 29 features (frequency components from 6 to 36 Hz with a length of 2 Hz and an overlap of 1 Hz) was used for the full description of the EEG band power during motor execution for each 1 s segment.

All patterns were labeled twice for the classification of either ERD or ERS against all other brain activity. The ERD patterns during movement execution where labeled as class 1 from $t = 2.5$ to 3.5 s, all others patterns were labeled as class 0. In a similar way, ERS patterns after movement ($t = 4$–5 s) were labeled as class 1.

Fig. 1 shows the labeling procedure for each trial.

Information related to motor execution (ERD or ERS) is labeled as class 1. This period is from now on referred to as intentional control period (ICP). As a consequence, the rest of the time is referred to as non-intentional control period (NICP). Because ERD and post-movement ERS share slightly different frequency components (Müller-Putz et al., 2007b) and only the later coincides with the excitability level of motor cortex neurons, ERD and ERS can be described as mutually exclusive.

2.3. Pattern recognition

Two independent classifiers were trained for individual detection of ERD or ERS within their respective ICP. Support vector machines (SVM) with Gaussian kernels were used for this task. The SVM are binary classifiers that find an optimal hyperplane to separate classes by maximizing the margin between the hyperplane and the patterns that define the border in both distributions (support vectors). The library lib-SVM libsvm in combination with the Matlab interface from the BioSig Project (Schlögl et al., 2007) were used for the implementation of the SVM.

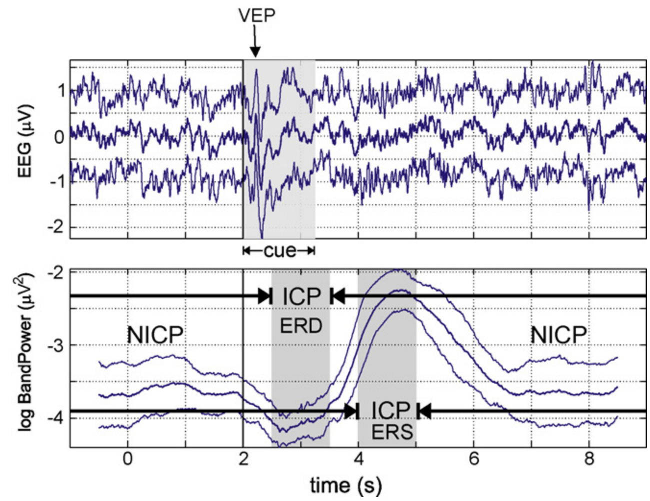

Fig. 1. Labeling procedure and period definition. Logarithmic band power features were obtained from trials of 10 s length, for ERD classification class 1 (and the intentional control period, ICP) is defined from $t = 2.5$ to 3.5 s; class 1 for ERS classification is defined from $t = 4$ to 5 s. The rest of the time is referred as non-intentional control period (NICP). Is important to remark that: (i) the first 500 ms after the cue presentation ($t = 2$ s) evoke a visual potential and (ii) the transition between ERD and ERS is considered as NICP for both phenomena. (Up: average EEG, bottom: average band power from all bands used as features; both plots show the average (bold line) ± S.D. Subject s1 is used as example.)

2.3.1. Training

The selection of hyperparameteres for the SVM was conducted in three steps. First, patterns from one (training) run were used to train a classifier. The performance of this classifier was estimated using a 10-fold cross-validation over the training data. This classifier was tested with the patterns from a second (testing) run. The true positive rate (TPR) and false positive rate (FPR) from this test were computed and stored for parameter selection (the performance of the classifier depends on the regularization parameter C and the width of the kernel σ). After testing all combinations of parameters (with logarithmic steps in the range {0:2} for each variable) two measures of the performance (TPR and FPR values associated with each combination of parameters) regarding the analysis of receiver operating characteristics (ROC) curve information were available. These two measurements were combined into a single one using the Youden index ι (Sokolova et al., 2006)

$$\iota = \mathrm{TPR} - \mathrm{FPR}, \tag{1}$$

the parameters $C_{\max(t)}$ and $\sigma_{\max(t)}$, associated with the global maximum ι, were selected to train a new SVM.

After this step a new SVM was trained with $C_{\max(t)}$ and $\sigma_{\max(t)}$ and the patterns from the training run. The SVM model was also trained for posterior class probability estimation (Chang and Lin, 2001; Wu et al., 2004) that uses 5-fold cross-validation implemented in lib-SVM. Only the Gaussian kernel was used with a complete search for hyperparameters, as it has been reported that under this conditions there is no need to consider SVM with linear kernels (Keerthi and Lin, 2003). To this end only two runs are used for parameter selection and training of the classifiers, the generalization capabilities of the SVM under this scheme were tested by computing all possible combinations of two runs for training/testing.

2.3.2. Testing

The trained SVMs were used to compute the ERD and the ERS posterior probabilities for patterns obtained from a validation run (a third run not used to train/test the classifier). This run was described using the same number of logarithmic band power features for time segments of 1 s (250 samples) shifted only one sample forward, respectively, to the immediate anterior segment. In this way the simulation of an online asynchronous system was achieved.

2.3.3. Performance measurements

The probability output of the classifiers was additionally post-processed with three simple parameters. One threshold, a dwell time and a refractory period (Townsend et al., 2004) were used. ROC analysis over the threshold value was conducted and the values for the dwell time (62 samples) and for the refractory period (500 samples) were picked by hand. These two parameters allow the system to make fast decisions (dwell time = 248 ms) and limits the number of detections during ICP interval. Since ERD or ERS may be present at any time after the cue presentation, the ICP was extended up to 2 s from $t = 2.5$ to 4.5 s for ERD and $t = 3.5$ to 5.5 s for ERS. All results reported in this paper were obtained from the ROC curves as the maximum TPR associated with a FPR ≤ 0.1.

TPR and FPR were computed as detection of events and not on a sample-by-sample basis. A *true positive control event* (TPIC) is regarded as any detection (number of samples over the threshold equal to the dwell time) during an ICP and a *false positive control event* (FPIC) is any detection outside an ICP.

$$\mathrm{TPR} = \frac{\mathrm{TPIC}}{N_{\mathrm{TPIC}}} \tag{2}$$

$$\mathrm{FPR} = \frac{\mathrm{FPIC}}{N_{\mathrm{FPIC}}} \tag{3}$$

where N_{TPIC} is the number of TPIC (equal to the number of ICP since only one detection is allowed) and N_{FPIC} = total number of samples/(dwell time + refractory period). All runs used a random inter-trial interval that leads to differences in the number of samples; in this study the values of the number of events are $N_{\mathrm{TPIC}} = 30$ and $N_{\mathrm{TPIC}} \simeq 110$.

2.3.4. Π-rule for combination of motor-related information

Information about actual movement and its ending was combined to enhance the accuracy and minimize false negatives. Both classifiers for ERD and ERS were combined under the following assumptions:

1. ERD is present in all motor execution tasks.
2. If an ERS is present, it is always after an ERD.
3. Classifications of ERD and ERS are independent of each other.

These assumptions allow us to compute the joint probability as the product of the independent event probabilities: $P(\mathrm{ERD}, \mathrm{ERS}) = P(\mathrm{ERD})P(\mathrm{ERS})$, where $P(\mathrm{ERD})$ and $P(\mathrm{ERS})$ are the estimated probabilities for each event. This combination was called Π-rule. However, these assumptions make the co-ocurrance of both events impossible. This problem is overcome by delaying $P(\mathrm{ERD})$ by 1 s to match the ICP for ERS during testing and then computing the product of both probabilities. It is important to mention that detections before $t = 3.5$ s cannot be regarded as motor activity due to the delay and the time of the cue. The performance was measured as described above.

2.4. ERD/ERS maps

Time–frequency maps were computed for each subject using the data from all three runs. To obtain an ERD/ERS map an analysis of overlapping frequency bands between 6 and 36 Hz using a bandwidth of 2 Hz was performed. Significant ($p < 0.05$) band power decrease or increase (ERD/ERS) with respect to the reference ($t = 0.5$–1.5 s) was determined using a bootstrap algorithm. For further details see Graimann et al. (2002). The mean ($\bar{X}$) and median ($\tilde{X}$) maps were computed to show the general behavior of the patterns.

3. Results

3.1. ERD/ERS information

Fig. 2 shows the ERD/ERS maps obtained for all subjects. The maps show the ERD phenomenon shortly after the cue presentation at $t = 2$ s and the presence of a beta rebound (ERS) around $t = 4$ s. The time–frequency localization of ERD/ERS is clearly identified with an ERD in slightly higher frequency components than ERS, matching the definitions of ICP for training and testing. From the analysis of these maps, few frequency components could be selected to tune the pattern description for each individual subject. In this work a wide pattern description and no feature selection were used to let the SVM learn the differences between ERD/ERS and EEG for every subject and to allow them to automatically adjust to the intra-subject variability (non-relevant features are given a small weight during maximization of the margin for the SVM).

Fig. 3(a) shows the probability output for a single trial with classifiers based on ERD ($C_{P(\mathrm{ERD})}$) and ERS ($C_{P(\mathrm{ERS})}$). The signal from the $C_{P(\mathrm{ERS})}$ is smooth while the output for $C_{P(\mathrm{ERD})}$ presents a large variability along the trial length. Both outputs show some reactivity to patterns from other segments (brain activity), specially for the $C_{P(\mathrm{ERD})}$ in the 500 ms interval after the cue presentation due to the visual evoked potential. Fig. 3(b) shows the result of applying the Π-rule to the same trial (Fig. 3(b) is the combination of the probabilities in Fig. 3(a)). The reactions in other time segments are minimized and the probability at the ICP is the same as $C_{P(\mathrm{ERD})}$ modulated in amplitude by $C_{P(\mathrm{ERS})}$.

3.2. Performance

Table 1 shows the TPR and FPR values (mean ± S.D.) obtained from all combinations of train/test/validate runs for each subject and the grand average for these combinations. The highest individual performance is achieved in all cases for ERS classification with TPR values over 0.52 and a grand average of 0.74 ± 0.21. A two tailed *t*-test for repeated measurements was applied to the results of each subject (combinations of train/test/validate) showing no significative differences ($p \geq 0.05$) for the combination of classifiers with the Π-rule (C_{Π}) and the ERS classification ($C_{P(\mathrm{ERS})}$). Fig. 4 shows an example of the ROC analysis and the selection of TPR and FPR.

It was found that for ERD values between 0.20 and 0.30 (subjects s2, s3, s4 and s7), C_{Π} presents a slight improvement. This tendency was observed in all cases where a particular combination of train/test/validate runs achieved similar values. However, all those changes are below 0.03 and are not significant ($p \geq 0.05$) in all cases except for s7, where the improvement is significant ($p = 0.03$) and around 0.10.

In the cases of $C_{P(\mathrm{ERS})}$ and C_{Π} the maximum time for detection is $t = 3.5$ s relative to the cue and the fastest detection possible is $t = 1.748$ s (ICP start + dwell time = 1.5 s + 0.248 ms). This interval allows an information transfer rate (ITR) between 17.14 and 34.32 bits/min (when TPR = 1) using the definition given by Wolpaw et al. (1998):

$$I = \log_2 N + P \log_2 P + (1 - P)\log_2 \frac{1 - P}{N - 1} \tag{4}$$

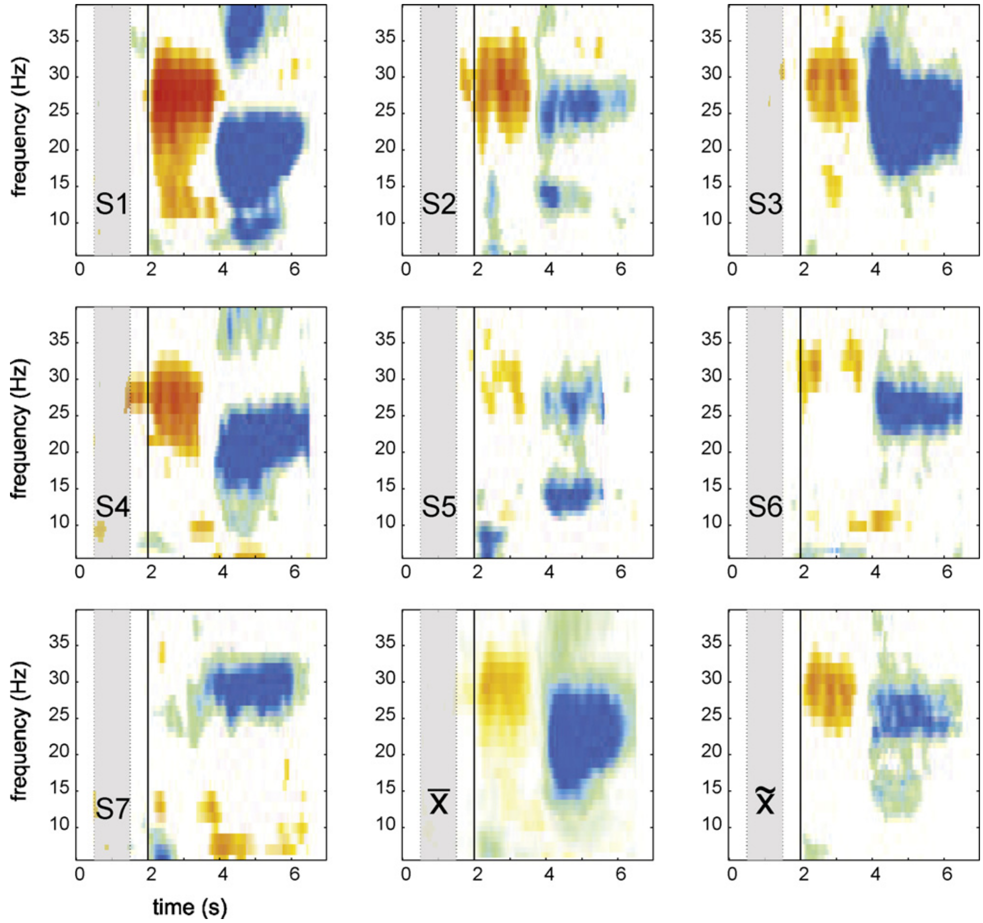

Fig. 2. ERD/ERS maps. The relevant changes in amplitude of each band are described in each map for individual subjects (s1–s7), the last two maps ($\bar{X}$ and $\tilde{X}$) represent the mean and median of all ERD/ERS maps, respectively.

where P is the classification accuracy and N the number of control states. This definition was deduced from the mutual information (MI) formulation and then simplified for equal probabilities and equal performance of the classifiers. These conditions do not hold in current systems, making this measurement not suitable for real life applications. Fatourechi et al. (2006) have recently applied the definition of mutual information for an asynchronous BCI with the addition of information related to the differences in probabilities and the performance of the classifier during NICP, showing that ITR can be formulated for an asynchronous BCI.

For this ITR, the formulation used in this results is

$$I(X, Y) = -\sum_{j=1}^{2} P(y_j)\log_2\ P(y_j) + \left(\sum_{i=1}^{2}\sum_{j=1}^{2} P(x_i)P(y_j|x_i)\log_2\ P(y_j|x_i)\right) \tag{5}$$

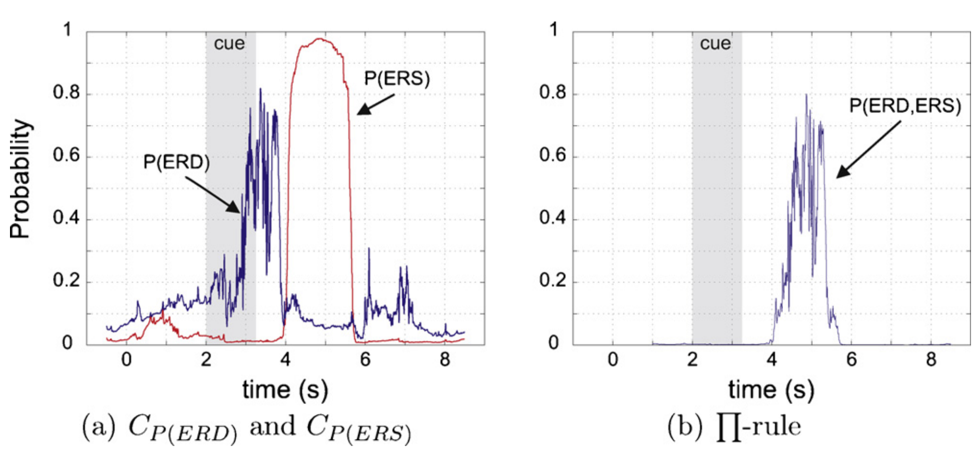

Fig. 3. Single trial ERD/ERS classification. The probability output from the SVM and individual event classification (a) for a single trial and the Π-rule (b) is shown above. The oscillations or variability in the resulting output are due to the ERD classification. Note the reduction of 'noise' in the probability output of time segments not related with motor execution.

Table 1
Individual performance

ID	$C_{P(\mathrm{ERD})}$		$C_{P(\mathrm{ERS})}$		C_{Π}	
	TPR	FPR	TPR	FPR	TPR	FPR
s1	0.34 ± 0.05	0.08 ± 0.01	0.97 ± 0.05	0.03 ± 0.02	0.92 ± 0.07	0.03 ± 0.03
s2	0.28 ± 0.13	0.08 ± 0.01	0.61 ± 0.10	0.07 ± 0.02	0.62 ± 0.14	0.07 ± 0.02
s3	0.23 ± 0.17	0.05 ± 0.03	0.94 ± 0.05	0.04 ± 0.04	0.95 ± 0.05	0.04 ± 0.02
s4	0.20 ± 0.08	0.07 ± 0.03	0.83 ± 0.12	0.04 ± 0.03	0.86 ± 0.14	0.06 ± 0.02
s5	0.12 ± 0.12	0.05 ± 0.03	0.54 ± 0.14	0.07 ± 0.02	0.49 ± 0.19	0.08 ± 0.02
s6	0.11 ± 0.08	0.05 ± 0.04	0.79 ± 0.12	0.08 ± 0.01	0.73 ± 0.13	0.07 ± 0.03
s7	0.22 ± 0.14	0.08 ± 0.02	0.52 ± 0.20	0.06 ± 0.02	0.64 ± 0.17	0.07 ± 0.02
$\bar{X}$	0.21 ± 0.12	0.06 ± 0.03	0.74 ± 0.21	0.06 ± 0.03	0.74 ± 0.20	0.06 ± 0.03

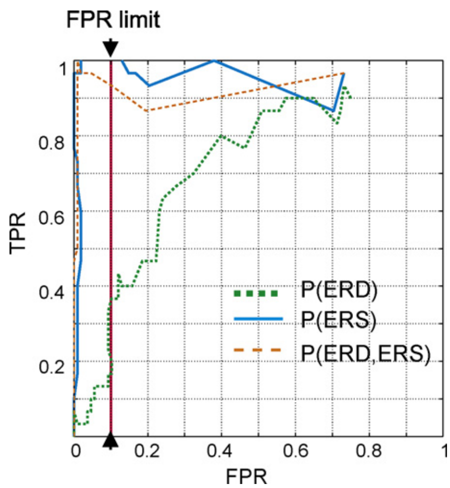

Fig. 4. TPR and FPR. A ROC curve for one of the combinations train/test/validate for subject s1 is presented as an example of the performance and the selection of results in this paper (operation point). After the ROC analysis the results are selected as the maximum TPR possible with a maximum of 0.1 FPR. In this case, and in general both results for $C_{P(\mathrm{ERS})}$ and C_{Π} are the same, however, the classifier performance is clearly changed. This can be seen from the shape of the ROC curves, additional values of area under ROC curve and changes in the maximum in the Youden index (ι).

where X is the transmitter (in this case the EEG and brain states), Y the receiver (classification system), the indices i and j regard the states: 1 = intentional control and 2 = no intentional control, $P(y_j)$ is the probability of the system (classifier) to generate an output of the state y_j (equal to 0.5 for unbiased classifiers), $P(x_i)$ is the class probability ($P(x_1) \ll P(x_2)$) and $P(y_j|x_i)$ is the probability of classifying as j an event i.

Table 2 shows the mean values of ITR with the new formulation for each subject and the classifiers based on ERS and the Π-rule. All values of ITR are above 8.00 bits per minute (bits/min) for an average detection time of 2.6 s and individual TPR and FPR values.

Table 2
Information transfer rate (bits/min) obtained with the classifiers: $C_{P(\mathrm{ERS})}$ and C_{Π}

ID	$\mathrm{ITR}_{P(\mathrm{ERS})}$	ITR_{Π}
s1	18.57	15.5
s2	8.22	8.24
s3	16.49	16.65
s4	12.10	12.07
s5	8.15	8.25
s6	9.79	9.20
s7	8.85	8.45
$\bar{X}$	11.74 ± 4.22	11.19 ± 3.61

4. Discussion

Even though no significative differences were found between $C_{P(\mathrm{ERS})}$ and C_{Π} (see Section 3.2), it can be speculated that there is considerable potential of improvement in single trial classification with this combination rule and when intra-individual optimization of the dwell time and refractory period is performed.

The time–frequency maps in Fig. 2 display some degree of inter-subject variability. Besides this variability, a dense ERS is present in all subjects in contrast to a sparse ERD in some subjects. These findigs are in accordance with the performance results (Table 1) where the highest performance for individual ERD/ERS pattern detection is obtained with the classifier based on ERS.

The SVM showed a stable performance with the training/testing scheme presented here. This results were expected although it has been reported (Blankertz et al., 2007) that the inclusion of more data (old and new) improves the performance of the classifier. In this work all data were recorded within the same day and a robust classifier was used. The high dimensionality of feature vectors does not represent a problem. Parameter selection for the SVM is a time consuming task.

Two recently published reports also present results on the research and development of BCI systems based on the dynamics of brain oscillations. In Fatourechi et al. (2008) a fully automated self-paced BCI is proposed. The authors described a method for feature extraction, classification and optimization to detect a cue-based finger flexion. Features were extracted from movement-related potentials and power changes in mu and beta rhythms. Classification was achieved with a set of SVM and a hybrid genetic algorithm to optimize the system parameters. With 18 bipolar channels the performance achieved was around TPR = 0.56 in average for the analyzes made in four healthy subjects.

Bai et al. (2008) reported on a beta-rhythm BCI where six healthy subjects performed several sessions of wrist motor execution and motor imagery. EEG was recorded using 29 electrodes and 16 frequency bins for band power computation for feature selection. Thereafter with a single Laplacian channel and a subject-specific power value the motor execution and motor imagery were classified, respectively. All subjects achieved successful control of a video game with an information transfer rate between 10 and 12 bits/min.

The methods presented in this work and the novel combination of information with the Π-rule achieved higher results in the classification of motor execution and information transfer rate in the offline analyses even though no optimization of the features or the patterns were applied. In this sense, our approach presents promising results for the use at home of a BCI system, using five electrodes in one single channel and a general paradigm for training the classifiers. Moreover, a similar set of features was used for every subject and just two runs (roughly 15 min) are needed to find the parameters of the classifier. Possible applications are games like the one presented in Bai et al. (2008) or Müller-Putz et al. (2007a). Improvements in the performance of the methods described here are expected with the addition of parameter optimization methods.

5. Conclusions

It was demonstrated that a single Laplacian derivation is suitable for detection of brisk foot movement in ongoing EEG. For the first time information related to brain signal dynamics during and after motor execution was combined to improve the performance of single trial classification. An acceptable transfer rate can be achieved after just three training sessions (two for set up the classifier and one for validation). Future work will include feature selection and the optimization of the dwell time and refractory period and test on motor imagery data.

Acknowledgments

This work was carried out as part of the EU project PRESENCCIA (IST-2006-27731) and supported by the "Steiermärkische Landesregierung" project GZ: A3-16 B 74-05/1, by the Austrian "Allgemeine Unfallversicherung AUVA" and Lorenz Böhler Gesellschaft. We thank Dr. R. Scherer for the valuable discussions in this study.

References

Bai O, Lin P, Vorbach S, Floeter MK, Hattori N, Hallett M. A high performance sensorimotor beta rhythm-based brain–computer interface associated with human natural motor behavior. J Neural Eng 2008;5:24–35.
Birbaumer N, Ghanayim N, Hinterberger T, Iversen I, Kotchoubey B, Kübler A, et al. A spelling device for the paralysed. Nature 1999;398:297–8.
Blankertz B, Dornhege G, Krauledat M, Müller KR, Curio G. The non-invasive Berlin brain–computer interface: fast acquisition of effective performance in untrained subjects. Neuroimage 2007;37:539–50.
Chang CC, Lin CJ. LIBSVM: a library for support vector machines; 2001. Software available at <http://www.csie.ntu.edu.tw/~cjlin/libsvm>.
Chen R, Yassen Z, Cohen LG, Hallett M. The time course of corticospinal excitability in reaction time and self-paced movements. Ann Neurol 1998;44:317–25.
Ehrsson HH, Geyer S, Naito E. Imagery of voluntary movement of fingers, toes, and tongue activates corresponding body-part-specific motor representations. J Neurophysiol 2003;90:3304–16.
Fatourechi M, Mason S, Birch G, Ward R. Is information transfer rate a suitable performance measure for self-paced brain interface systems? Proc IEEE Int Symp Signal Process Inf Technol 2006.
Fatourechi M, Ward RK, Birch GE. A self-paced brain–computer interface system with a low false positive rate. J Neural Eng 2008;5:9–23.
Gerardin E, Sirigu A, Lehéricy S, Poline JB, Gaymard B, Marsault C, et al. Partially overlapping neural networks for real and imagined hand movements. Cereb Cortex 2000;10:1093–104.
Graimann B, Huggins JE, Levine SP, Pfurtscheller G. Visualization of significant ERD/ERS patterns multichannel EEG and ECoG data. Clin Neurophysiol 2002;113:43–7.
Hari R. Action–perception connection and the cortical mu rhythm. In: Neuper C, Klimesch W, editors. Event-related dynamics of brain oscillations. Progress in brain research, vol. 159. Amsterdam: Elsevier; 2006. p. 253–60.
Hjorth B. An on-line transformation of EEG scalp potentials into orthogonal source derivations. Electroencephalogr Clin Neurophysiol 1975;39:526–30.
Keerthi S, Lin CJ. Asymptotic behaviors of support vector machines with Gaussian kernel. Neural Comput 2003;15(7):1667–89.
Leeb R, Friedman D, Müller-Putz GR, Scherer R, Slater M, Pfurtscheller G. Self-paced (asynchronous) BCI control of a wheelchair in virtual environments: a case study with a tetraplegics. Comput Intell Neurosci 2007:79642.
Lotze M, Montoya P, Erb M, Hülsmann E, Flor H, Klose U, et al. Activation of cortical and cerebellar motor areas during executed and imagined hand movements: an fMRI study. J Cogn Neurosci 1999;11:491–501.
Müller GR, Neuper C, Rupp R, Keinrath C, Gerner HJ, Pfurtscheller G. Event-related beta EEG changes during wrist movements induced by functional electrical stimulation of forearm muscles in man. Neurosci Lett 2003;340:143–7.
Müller-Putz GR, Scherer R, Pfurtscheller G. Game-like training to learn single switch operated neuroprosthetic control. In: Int. Conf. Adv. Comput. Entertainment Technol. Workshop. BrainPlay'07: playing with your brain (brain–computer interfaces and games); 2007a. p. 49–51.
Müller-Putz GR, Zimmermann D, Graimann B, Nestinger K, Korisek G, Pfurtscheller G. Event-related beta EEG-changes during passive and attempted foot movements in paraplegic patients. Brain Res 2007b;1137:84–91.
Neuper C, Müller GR, Kübler A, Birbaumer N, Pfurtscheller G. Clinical application of an EEG-based brain–computer interface: a case study in a patient with severe motor impairment. Clin Neurophysiol 2003;114:399–409.
Neuper C, Pfurtscheller G. Evidence for distinct beta resonance frequencies in human EEG related to specific sensorimotor cortical areas. Clin Neurophysiol 2001;112:2084–97.
Pfurtscheller G, Lopes da Silva FH. Event-related EEG/MEG synchronization and desynchronization: basic principles. Clin Neurophysiol 1999a;110:1842–57.
Pfurtscheller G, Lopes da Silva FH, editors. Event-related desynchronization, handbook of electroencephalography and clinical neurophysiology. Amsterdam: Elsevier; 1999b. p. 6.
Pfurtscheller G, Müller-Putz GR, Pfurtscheller J, Rupp R. EEG-based asynchronous BCI controls functional electrical stimulation in a tetraplegic patient. Eur Assoc Signal Process J Appl Signal Process 2005a;19:3152–5.
Pfurtscheller G, Neuper C, Brunner C, Lopes da Silva FH. Beta rebound after different types of motor imagery in man. Neurosci Lett 2005b;378:156–9.
Salmelin R, Hamalainen M, Kajola M, Hari R. Functional segregation of movement related rhythmic activity in the human brain. Neuroimage 1995;2:237–43.
Scherer R, Schlögl A, Lee F, Bischof H, Janša J, Pfurtscheller G. The self-paced Graz brain–computer interface: methods and applications. Comput Intell Neurosci 2007:79826.
Schlögl A, Brunner C, Scherer R, Glatz A. BioSig: an open-source software library for BCI research. In: Dornhege G, Millán J, Hinterberger T, McFarland DJ, Müller KR, editors. Towards brain–computer interfacing, vol. 20. MIT Press; 2007. p. 347–58.
Sokolova M, Japkowicz N, Szpakowicz S. Beyond accuracy, *F*-score and ROC: a family of discriminant measures for performance evaluation. Berlin/Heidelberg: Springer; 2006. p. 4304.
Thorpe J, van Oorchot P, Somayaji A. Pass-thoughts: authenticating with our minds. In: Proc new Secur paradigms workshop; 2005.
Townsend G, Graimann B, Pfurtscheller G. Continuous EEG classification during motor imagery-simulation of an asynchronous BCI. IEEE Trans Neural Syst Rehabil Eng 2004;12:258–65.
Wolpaw J, Birbaumer N, McFarland DJ, Pfurtscheller G, Vaughan TM. Brain–computer interfaces for communication and controls. Clin Neurophysiol 2002;113:767–91.
Wolpaw J, McFarland D, Pfurtscheller G. EEG-based communication: improved accuracy by response verification. IEEE Trans Rehabil Eng 1998;6:326–33.
Wu T, Lin C, Weng R. Probability estimates for multi-class classification by pairwise coupling. J Mach Learn Res 2004;5:975–1005.